Journal of Micromechanics and Microengineering

https://doi.org/10.1088/1361-6439/ab0720

A methodology for 3D geometrical characterisation of microfluidic channels using optical microscopy

F. Medeossi[1], N. Senin[2,3], M. Balcon[1], S. Carmignato[4], E. Savio[1], L. Blunt[5]
[1]*DII, Dip. di Ingegneria Industriale, Università di Padova, Italy*
[2]*Dip. di Ingegneria Industriale, Università di Perugia, Italy*
[3]*Faculty of Engineering, University of Nottingham, UK*
[4]*DTG, Dip. di Tecnica e Gestione dei Sistemi Industriali, Università di Padova, Italy*
[5]*CPT, Centre for Precision Technologies, University of Huddersfield, UK*

Abstract
In manufactured microfluidic channels, geometrical imperfections resulting from the manufacturing process are challenging in terms of reliability and functionality of the microfluidic device. In this work, a methodology for the geometrical and dimensional characterization of microfluidic channels using quantitative 3D optical microscopy is proposed. The methodology is based on a holistic approach including the identification of functionally relevant geometrical features and critical dimensions at design stage, as well as the related verification process at the manufacturing stage. At design stage, the critical geometrical characteristics are identified on the basis of their relation with the performance of the microfluidic device. Verification is based on a novel methodology in which measurement results collected by a surface topography measuring instrument are processed on the basis of concepts and procedures commonly applied to data generated by a coordinate measuring system.
The method is presented using as an example the characterisation of a microfluidic channel realized by soft lithography and constituting part of a membrane micro valve. The geometry of the microfluidic channel is acquired by using an imaging confocal microscope.

Keywords: Microfluidics, micro manufacturing, imaging confocal microscope, dimensional characterization, feature extraction

1 Introduction
Micro-valves are fundamental for the fluid-flow control on a given micro-fluidic platform. These elements enable liquids to be controlled on-chip and they are the key to realizing large-scale microfluidics integration. A sizeable amount of research work has been carried out on the actuation methods, fabrication principles and different geometries (Oh 2015, Whitesides 2006).
Multilayer soft lithography is one of the most developed technologies for the fabrication of pneumatically driven micro-valves (McDonald and Whitesides 2002). In multilayer soft lithography, a soft polymer, such as polydimethylsiloxane (PDMS), is cast onto a mould that contains a micro fabricated relief or engraved pattern. The full fabrication process, from the design to its implementation leading to the final product, can be developed within one day (Unger et al. 2000, Eddings et al. 2006).
A basic push-down micro-valve is composed of two elastomeric layers: one contains channels for flowing liquids (flow layer) whilst the other contains channels that deflect the membrane valve into the flow channel and stop liquid flow when pressurized with air or liquid (control layer) (Unger et al.

2000, Studer et al. 2004). The working principle is presented in Figure 1: the increase of fluid pressure in the control flow leads to the collapse of the soft ceiling of the flow channel. This way, the fluid flow in the flow layer is interrupted (Figure 1.b). Three or more such devices, actuated in the correct sequence, can be used, for example, to realise a peristaltic pump.

A push-down micro-valve is realized joining three different parts: a commercial glass for microscopy, a PDMS flow layer (containing the channel for the main flow) and a PDMS control layer (containing the control channel).

The geometry of the channels is achieved by letting liquid PDMS solidify over a mould (the master) shaped as the negative of the channel. Choice of the process parameters used to obtain the master and the parts (mainly intensity of the ultraviolet light, exposure time and baking time of the master) is a critical step for ensuring the final geometry of the channels cross-section. After the control layer and the flow layer are produced, they are aligned and joined together with the glass through plasma bonding. Once the chip is assembled, the inlet and outlet holes are punched.

Several factors can lead to the valve failing its functional role, the most prominent being leakage of fluid from the flow channel and incomplete closure. These types of failure can be related to defective materials, presence of bubbles, incomplete bonding and incorrect geometrical and dimensional characteristics of the layers.

Traditionally, the individual parts are verified mainly through visual inspection by means of conventional 2D optical microscopy and scanning electron microscope (SEM) imaging. However, most of these inspections are only devoted to the identification of local defects in the material (bubbles, inclusions, lack of material). Instead, incomplete bonding between layers and incomplete closure of the flow channel are only detected at the last stage of the production process (i.e. at functional testing of the assembled valve). This is generally done by observing fluid leaking out of the sides of the channels and flowing into the gaps between the valve and fluid flowing through the channel, despite having applied the correct closing pressures.

More effective inspections aimed at understanding the actual 3D geometry of individual parts have the potential to reduce overall development and manufacturing costs (Savio et al. 2016). Specifically, for the valve assembly, a timely and comprehensive geometrical quality control of the individual parts could lead to avoiding the assembly, punching and verification of valves that would fail functional testing, thus greatly reducing production time and costs (Savio et al. 2012). As a matter of fact, although the production process is quite fast (a few hours), the steps of assembling and punching the parts are critical, as they require trained operators to perform e.g. accurate alignment of parts being assembled.

Different techniques are generally available for 3D geometrical characterisation of complex shaped parts. Coordinate metrology is the most widely adopted solution for dimensional and geometrical quality control in manufacturing industry, and consists on the collection of set of points on the surfaces to be inspected using e.g. a coordinate measuring machine (CMM) followed by data processing to obtain the information of interest (e.g. size, diameter, form error). Because of their widespread adoption, most standards on conformity assessment are designed for CMM measurements, and a large amount of information exists for quality assurance purposes (Hocken 2017). Despite the increasing availability of miniaturised probes and non-contact probing solutions, CMMs are inherently slow and limited in performance with accuracy at µm level when dealing with micro-parts (Carmignato et al. 2010). 3D stylus-based instruments and Atomic force microscopes (AFMs) are also used for quantitative measurements on micro-parts with nm resolution (Dixson 2018), and efforts have been made to make AFM-operation in dimensional verification more similar to CMMs, through the implementation of non-raster sampling strategies (Savio et al. 2007) and high aspect ratio calibration artefacts (Marinello et al. 2008). However, microfluidic channels of interest for this paper have dimensions of few hundreds of micrometres and made of deformable material; therefore, they cannot be measured reliably by contact probing devices or AFMs.

Non-contact instruments such as coherence scanning interferometers and confocal microscopes are available with resolutions up to sub-nm level, albeit they have been primarily designed for the characterization of surface texture (Leach 2011). When considering the use of such instruments for dimensional and geometric verification tasks, a few relevant aspects should be considered (Senin et al. 2013): unidirectional observation (no vertical/high-sloped surfaces or undercuts can be acquired), uniform sampling density with grid layout (which may be suboptimal since it may not

comply with the requirements of localized features) and rectangular acquisition areas (again potentially suboptimal with respect to measurand projected boundaries).
At the scale of interest, additional challenges are related to the relatively larger manufacturing imperfections; geometrical measurements are consequently more challenging (Hansen et al. 2006, Hansen et al. 2011). General methods to design inspection and verification procedures at micro scale using high-density point sets found in the literature (Senin et al. 2012a; Senin et al. 2013) are here further developed and specifically dedicated to the inspection and verification of microfluidic channels.
This work focuses on the geometrical quality control of push-down valves featuring channels with cylindrical shape. For this type of channel design, both aspect-ratio (depth over width) and curvature radius of the channel cross-section play a critical role in determining the correct functional behaviour of the valve (Prevedello et al. 2018). If the aspect-ratio is too high, the ceiling may not reach the base surface when collapsed. Well-designed cylindrical shapes allow a complete closure of the channel, while other shapes (e.g. rectangular cross-sections, see Figure 1.c) may not work, even for appropriate aspect ratios (e.g. Figure 1.d) (Unger et al. 2000).

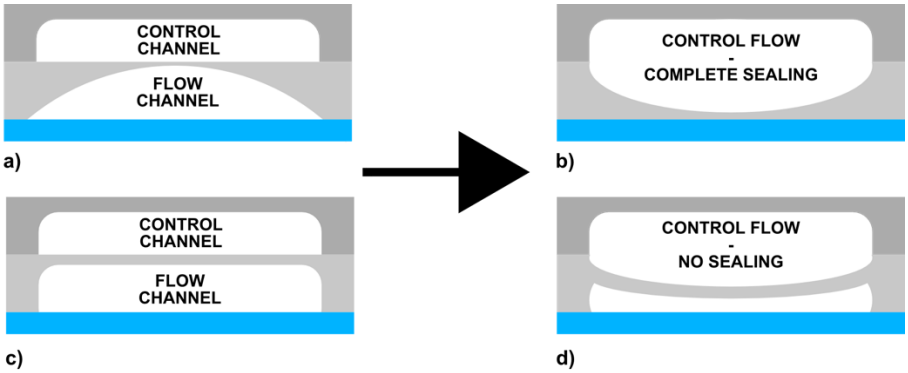

***Figure 1**: Architectures and working principles of push-down valves: (a) soft main channel with cylindrical cross-section; (b) channel collapsed under pressure closing the valve; (c) soft main channel with rectangular cross-section; (d) channel collapsed under pressure without closing the valve.*

The aim of this paper is to present a methodology for quantifying the geometrical and dimensional properties of a cylindrical channel. The proposed solution is not limited to inspecting an individual cross-section; instead, it aims at covering an entire area over the length of the channel. From a functional standpoint, an effective closure of the valve requires a long-enough portion of the flow channel surface to collapse properly onto the bottom surface, so the cross-section requirements must be consistently fulfilled over such length. Secondly, the manufacturing process (soft lithography) often has poor repeatability over the channel length, so checking for consistency of an individual position to obtain cross-section dimensional data may give unreliable indications of the neighbouring zones. Additionally, many sources of error affecting aspect ratio and out of roundness would be difficult to quantify, or even visualise, on a single cross-section profile, clearly this leads to the need to acquire an entire portion of the channel geometry.
It is also important to mention that additional benefits can be gained from the quantitative characterization of the flow channel geometry, in terms of an improved understanding of the manufacturing process capability, which in turn leads to the possibility of optimizing process parameters and designing improved process-aware product geometries.

2 Materials and methods

The proposed procedure consists of the following steps, illustrated in detail in the next sections:

- identification of the geometric properties to set as targets of the inspection process (i.e. critical dimensions);
- planning and execution of the data acquisition process (consistent with the inspection requirements);

- analysis and processing of the acquired data to compute the geometric properties of interest;
- assessment of conformance through comparison with the nominal references.

2.1. Identification of the critical dimensions

Three specific dimensions pertaining the micro-channel are considered relevant for successful fabrication of a valve: channel width, depth and radius of curvature (assuming the channel surface can be approximated to a cylindrical surface). Such channel dimensional attributes can be defined more rigorously by adopting the reference model illustrated in Figure 2. The model primarily consists of two datum surfaces: a planar surface ("top plane") and a cylindrical surface ("cylinder"), whose intersection generates the channel. In the inspection procedure, the two datum surfaces are supposed to be separately fitted, each to a properly partitioned subset of measured surface points. As the two fitting processes are independent, in general the datum cylinder axis will not be parallel to the datum top plane.

The critical dimensions are defined by considering a sectioning datum plane, orthogonal to the cylinder axis, cutting across the cylinder and top plane, named "orthogonal plane". At each position of the sectioning plane along the cylinder axis, the sectioning process generates a circle and a line, whose intersection in turn generates two points. Width is defined as the distance between such two points measured along the line; depth is defined as the distance between the line and the furthest circle point in the arc below the line, measured orthogonally to the line itself. Clearly, if the cylinder axis and top plane datum are not parallel, different values for width and depth will be obtained for each sectioning datum. In order to describe this misalignment between cylinder axis and top plane, the width and depth in the first and last section are reported, as well as the distance between the minimum and maximum value. The third relevant dimension is the channel radius of curvature; this is simply the radius of the fitted cylinder.

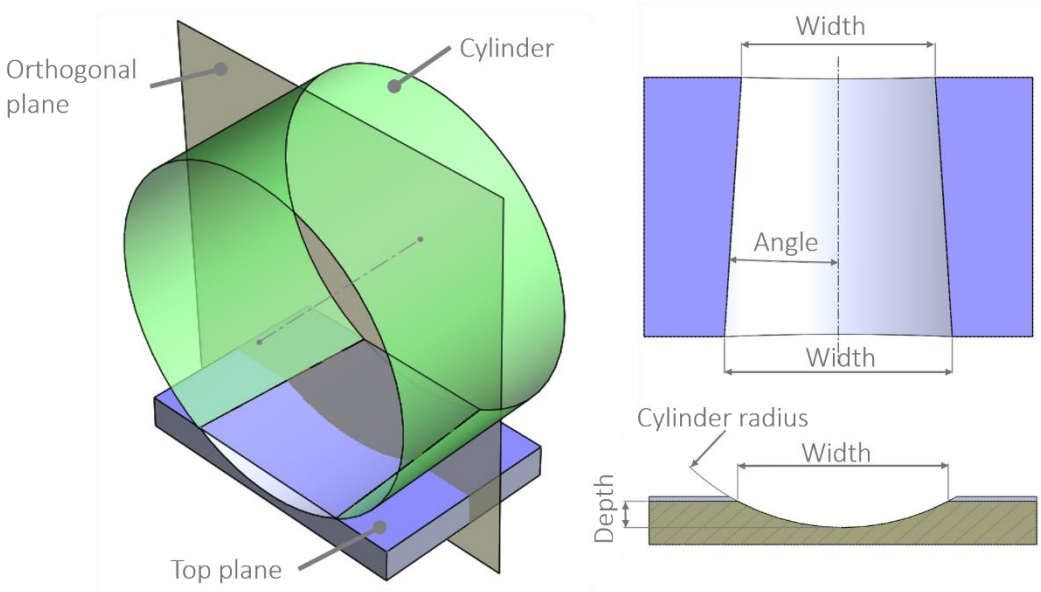

***Figure 2**: Representation of the reference model constituted of a plane and a cylindrical surface.*

2.2. Data acquisition process

The microfluidic channel is acquired by using an imaging confocal microscope (Sensofar Plu Neox) operating with blue light (λ_{blue} = 460 nm). The objective, a Nikon CFI-LU-EPI-P with 20x magnification, was selected considering two aspects:

- field of view (FOV): large enough to acquire the whole channel transverse topography without the need for stitching (i.e. collating) multiple FOVs, thus avoiding stitching errors;

- maximum measurable slope (limited by the numerical aperture (NA) of the objective) compatible with the need for measuring the sides of the channel.
The main instrument and objective technical specifications are summarised in Table 1.

Table 1: *Main instrument and objective technical specifications.*

Magnification	20x
NA	0.45
Maximum slope	21°
FOV (µm)	636.61 x 477.25
Spatial sampling	0.83 µm
Vertical resolution	< 20 nm

The instrument and objective were calibrated as follows: a flat mirror standard was used to correct aberration; a step height standard was used for vertical calibration (Silicon Depth Standard Type A1 - ISO 5436-1 – provided by SiMetricS). The calibrated value of depth is 10.24 µm ± 0.03 µm (*k* = 2).
For the specific test case, the output of the measuring instrument is a 768 × 576 matrix of height values, uniformly covering a rectangular acquisition area of 636.61 µm × 477.25 µm, with spatial sampling (i.e. distance between neighbouring points) of 0.83 µm × 0.83 µm. The resulting dataset can be analysed either as a range image or as a 3D point set (Senin et al. 2013).

2.3. Data processing to compute the critical dimensions

Following previous literature (Senin et al. 2012a; Senin et al. 2013), data processing consists of three main steps:
- pre-processing of the dataset (identification and processing of local measurement errors);
- identification of the relevant feature (channel);
- computation of the critical dimensions.

2.3.1. Preprocessing of the dataset

This step is aimed at identifying and processing errors which are typically found in optical, high-density areal measurements of surfacetopography, i.e. void points (i.e. non-measured points), and measurement artefacts.
Void points correspond to missing local data as not enough information has been received by the sensor (Medeossi 2018). At the microscale, with optical techniques such as confocal microscopy, used in this work, voids are frequently found in correspondence to high local slopes, deep/narrow recesses, and/or unfavourable combinations of local material properties. Void points for example are visible in Figure 3. For the purposes of solving dimensional metrology problems, void points are better left untouched (Senin et al, 2013), since the alternative, i.e. filling by interpolation of valid neighbours, may introduce an additional error source which may compromise/skew the computation of the critical dimensions.

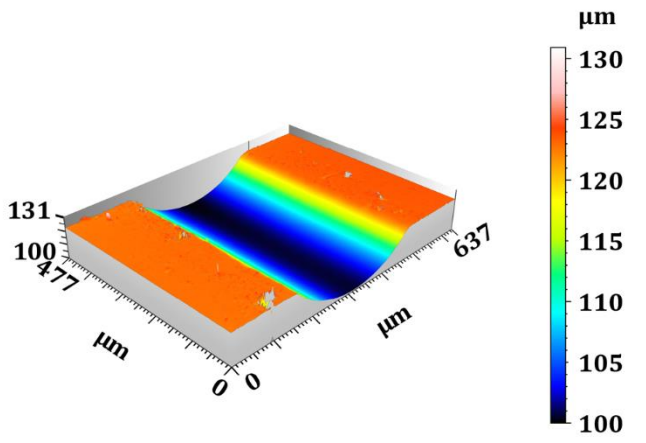

Figure 3*: Example of a microchannel measurement result with the presence of void points.*

Measurement artefacts are alterations in acquired surface data resulting from localised significant increases of measurement error going undetected by the instrument itself, and thus could not "voided". These artefacts often manifest themselves as significant peaks and pits and are called "bat wings" in the literature. They can result from phenomena such as focus hunting at steps and slopes, or material optical property inconsistencies. [Leach et al 2012]. Measurement artefacts are particularly hard to identify because they can be typically spotted only by observation of significant departures from the expected local topography (which implies some previous knowledge of the measured topography) and/or from the detection of specific signature patterns (Senin et al. 2012). On the contrary, when the topography is particularly irregular, measurement artefacts may be easily mistaken for actual topographic formations. In this work, measurement artefacts have been isolated by applying a method described in previous work (Senin et al. 2013), where they are identified as outliers by computing the difference between the local measurement values and a locally smoothed version (moving median) of the same region. The result of the outlier detection process for the microfluidics channel is illustrated in Figure 4. For the specific test case, optimal results are obtained by computing the median on a 9x9 pixels moving window by setting the threshold for outlier detection at four times the standard deviation of the residuals. Recognised measurement artefacts were turned into voids; then, voided regions are dilated (Gonzalez et al, 2007) with a circular structuring element (13 pixels radius) to compensate for outlier detection inaccuracies.

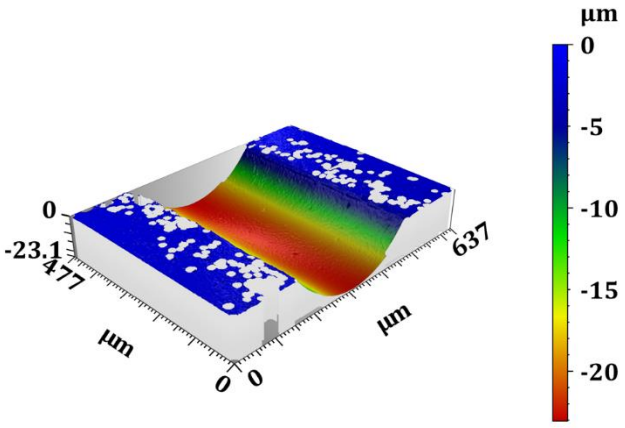

***Figure 4**: Result of the outlier detection process.*

2.3.2. Identification of the top plane and selective levelling of the topography

The identification of the top plane is based on the application of two combined thresholding methods. Firstly, a threshold on local slope is used to discriminate between coarsely horizontal regions and high-sloped ones. For the microchannel topography, both the top plane and a region at the bottom of the cylindrical channel are classified as low-sloped, while the channel side surfaces are tagged as high-sloped. The second threshold operation is on local height, and uses the notion that the bottom of the channel will be at lower height than the top surfaces. The second thresholding is only applied to the low-sloped regions recognised at the first step, and results in the channel bottom surface being eliminated from the low-sloped regions. At this point, the low-sloped regions only contain the top plane data.

Topography points recognised as belonging to the top plane are fitted to a mean plane via least-squares. Once the least-squares mean (LSM) plane fitted to the top-plane has been identified, a levelling operation is performed onto the entire topography, consisting of subtracting the heights of the LSM plane. This is a selective levelling operation, as opposed to a global levelling, because the LSM plane has been found by considering only the regions previously associated to the top plane. After levelling, the top plane topography is approximately horizontal, with zero mean height, and

thus can be used as a reference datum to compute channel depth, as illustrated later. The result of this procedure is shown in Figure 5a, where the extracted top plane is coloured in red.

2.3.3 Identification and fitting of the channel surface

The topography region corresponding to the microchannel is identified by taking the complement of the selection representing the top plane (obtained at the previous step). However, it is unadvisable to use the entire region for cylinder fitting. This is because the quality of confocal measurement decreases with slope (Balcon et al. 2012), thus the inaccuracy at the side walls of the microchannel may introduce significant error in the fitting result. To identify the bottom central region of the microchannel, a separate process is applied. Starting from the selective-levelled topography obtained as described in the previous section, a height thresholding operation at 50% of the topography vertical range is performed to isolate the bottom region of the channel (Figure 5b). Additional regions produced by thresholding, owing to other pits/recessed formations reaching depths below the threshold limit, are removed by identification of connected components (blob detection) and removal of the smallest ones (Gonzalez et al. 2007). Once the identified points belonging to the bottom of the channel have been extracted, they can be fitted to a cylindrical surface by a least-squares method. The adopted fitting algorithm is derived from previous work on cylinder fitting (Barker 2004), with modifications to turn the process into a weighted fitting. In this application, larger weights are given to points well below the depth threshold indicated earlier, since they are more likely to be associated to lower-sloped regions, thus more reliable to act as fitting references.

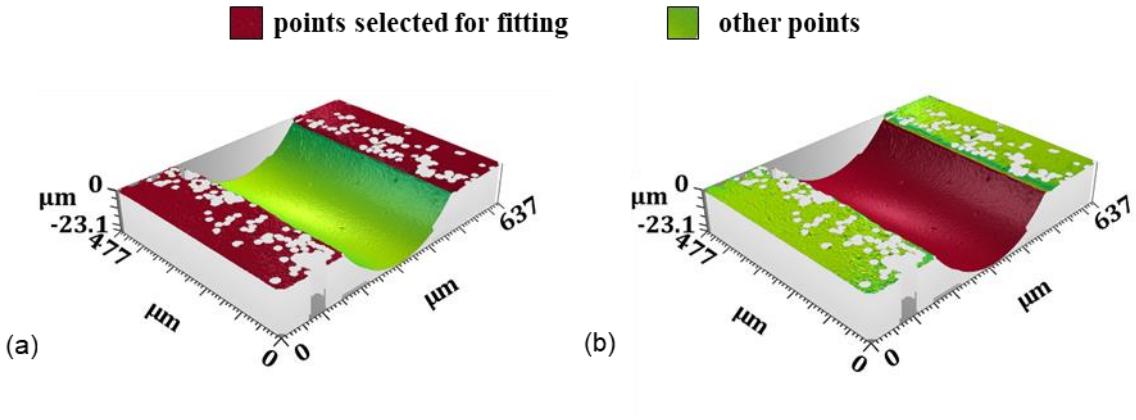

Figure 5*: Key moments of feature identification and fitting; a) the top plane is identified (highlighted in red) and aligned to the z = 0 plane (selective levelling); b) the central, bottom part of the microchannel is identified (in red) and used for cylinder fitting.*

2.3.4. Computation of the critical dimensions

As illustrated earlier, while channel radius of curvature is simply the radius of the fitted cylinder, channel width and depth are computed by sectioning the fitted cylinder and top plane with a third datum plane, orthogonal to the cylinder axis itself. As the sectioning plane is moved along the cylinder axis, different values for local width and depth are obtained (see Section 2.1). For the specific test case reported in this work, channel width and depth were obtained by arithmetic averaging over 10 cross-sections, spaced 47.8 µm along the cylinder axis, within the FOV.

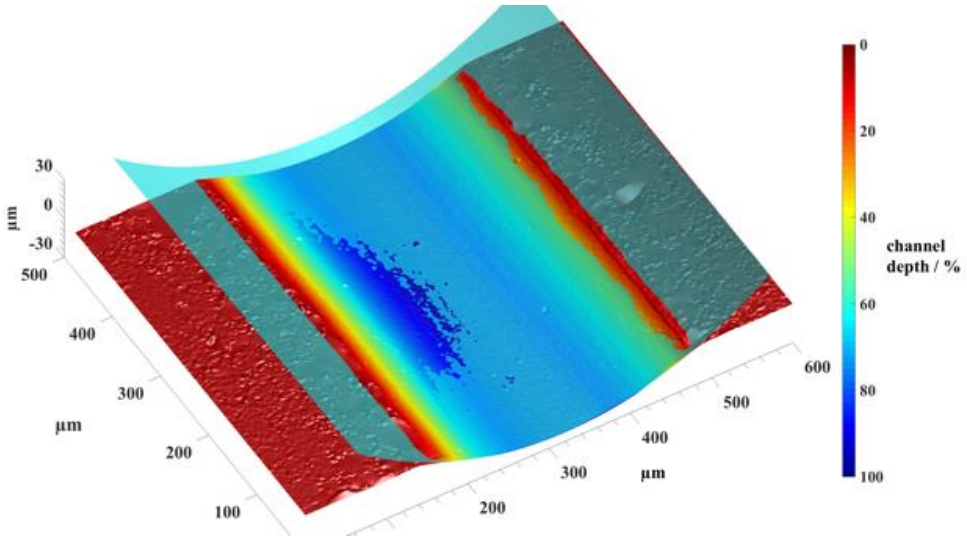

***Figure 6**: Visual reconstruction of the fitted cylinder, overlaid on top of the channel topography. The red-blue color map (reported in the color bar) refers to the relative depth of the channel (in percentage), whilst the cylinder surface is rendered in transparent cyan.*

Long-wavelength distortion as well as complex form deviation are not easily understood by looking at the results of the fitting procedure. In order to check the geometric regularity of the channel, residual plots are analysed instead.
Residuals are evaluated on the difference between the radius of the fitted cylinder and the perpendicular distance between the axis of the fitting cylinder and every single measured point. Root mean squared error (RMSE) and the maximum absolute difference between the fitted radius and the evaluated perpendicular distances are compared for a quantification of the regularity.

3. Results

The entire procedure was applied on a single sample, containing one channel, to demonstrate the feasibility of the proposed methodology. The complete areal topography measurement and data analysis process was repeated five times to investigate reproducibility. The measurement step was performed by manually placing the sample under the measuring instrument and using the same settings for each areal topography acquisition. Each data analysis process was comprised of computing depth and width over 10 cross-sections and calculating the average value on these sections and the difference between the maximum and minimum values. The results for 5 different measurements are summarized in table 2. Moreover, the average and the standard deviation of the 5 different measurements is reported in order to quantify the reproducibility of the method.

***Table 2:** Results for the 5 different measurement and data analysis repeats: values are expressed in µm.*

Meas. Num	***Radius***	***Depth***	***Width***
1	638.43	22.77	337.96
2	639.37	22.78	338.26
3	638.29	22.74	337.74
4	637.06	22.76	337.51
5	639.68	22.78	338.39
Avg.	638.6	22.77	338.0
Std.dev	1.0	0.01	0.4

The residuals plots are presented in Figure 7. A long-wavelength “barrel”-shaped form is highlighted by the plots.
Table 3 summarises the results obtained for the RMSE parameter and the maximum absolute distance between the measured points and the fitted cylinder. Both are computed by considering vertical distances between the actual channel points and the corresponding points on the fitted cylinder, within the region previously recognised by segmentation as belonging to the channel.

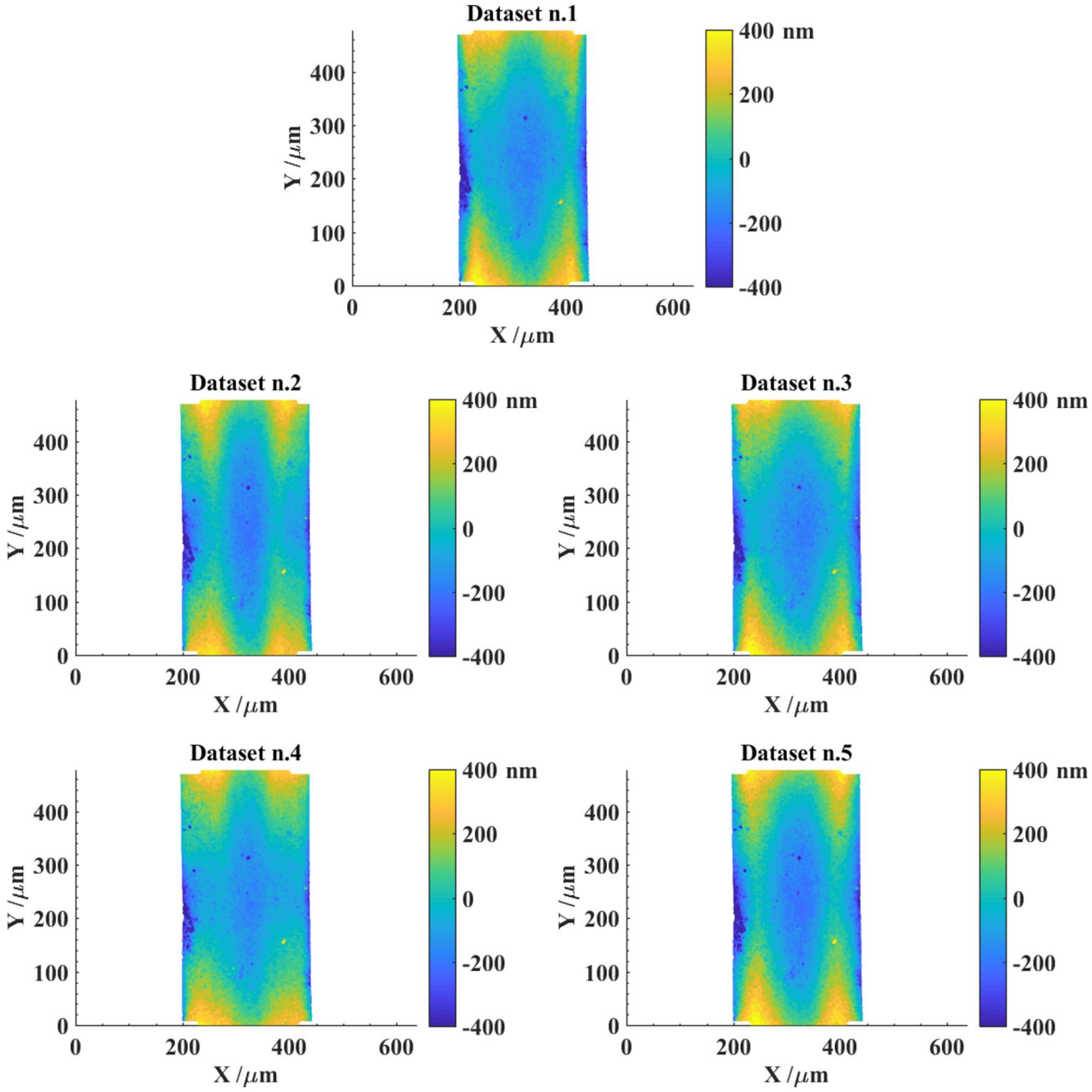

***Figure 7**: Residuals plots of the 5 different datasets.*

***Table 3:** Distribution of the actual points around the fitting cylinder. Values are expressed in μm.*

Meas. Num.	*RMSE*	*Maximum absolute distance*

1	0.14	1.33
2	0.14	1.34
3	0.15	1.35
4	0.13	1.34
5	0.15	1.38

4 Discussion

This paper has demonstrated the feasibility of geometrical characterisation of parts featuring micro-scale characteristics using quantitative optical microscopy, e.g. confocal microscopy, which can provide high-resolution 3D surface topography maps. While typically the datasets produced by these instruments are used to compute surface texture parameters (e.g. ISO 25178-2), as long as dedicated data analysis and processing procedures are developed, they can be used as the starting point to compute dimensional and geometric attributes of topographic features. The data processing methodology illustrated in the previous sections as it is applied to the microchannel test case, has been obtained by merging conventional surface metrology, image processing and point cloud analysis techniques. The approach is based on common efforts to develop dimensional metrology tools suitable for the micro scale (Jiang et al. 2007, Blunt et al. 2011, Senin et al. 2012b) and it is believed that many micro-fabricated parts can be characterized by a generalised application of this methodology. Some general issues need further investigation and are described in the following paragraphs.

Since the sample is measured optically using a single orientation of the sensor, the acquired surface data may not fully represent the real 3D geometry because undercuts (i.e. re-entrant surfaces) cannot be acquired. This limits the range of geometries that can be successfully characterised.

There are also limitations for high-sloped surfaces, as highlighted in the test case. For optical measurement, objectives with large magnification also feature high numerical aperture, thus increasing the maximum detectable slope and achieving higher vertical and lateral resolutions. Unfortunately, high magnification objectives present smaller fields of view and shorter measurement ranges, thus stitching (i.e. collating datasets in space) may be required. Current stitching techniques are still affected by significant error, which may hamper the reconstruction results. Another issue is computational time, which may become increasingly relevant in case of dense point sets. The longer the measurement and computational times, the less applicable is the solution to in-line inspection and verification. Micro computed tomography could be an alternative solution for 3D measurement tasks at micro scale provided that sufficient resolution is reached (De Chiffre et al. 2014, Ontiveros et al. 2012) however the restrictions of measurement time and data set size are significantly increased.

Moreover, image-processing techniques are easily available and well known in the world of imaging and their application to dimensional metrology, as shown in this work, is fairly straightforward. It is worth noting that errors originating from data processing such as filtering, levelling or erosion have to be accounted for in geometrical characterisation. For example, a median filtering operation will reduce outlier-type measurement artefacts; however, at the same time it will cause distortion in geometries and generally a smoothing of the surface. Thus, the application of median filtering in a geometric characterisation task should be carefully considered. Analogously, any algorithm of image processing, despite being immediately applicable given the equivalency between intensity images (e.g. grayscale) and height images / topographies, may introduce errors that are not relevant for a typical image processing tasks, but may become significant in dimensional metrology. Studies on the effect of data processing in dimensional measurement of sample are therefore necessary and may need to be optimised for individual measurement tasks.

5 Conclusions

A methodology to perform geometrical and dimensional characterisation of microfluidic channels using optical confocal microscopy has been proposed, following a holistic approach including the identification of functionally relevant geometrical features and critical dimensions at the design stage, as well as the related verification process at the manufacturing stage. The geometrical characterisation is based on a novel procedure in which measurement data collected by a surface topography measuring instrument using confocal microscopy are processed on the basis of concepts and procedures commonly used on data generated by a coordinate measuring system. The approach has been applied to the measurement of a microfluidic channel realized by soft lithography, part of a membrane micro valve. Quantitative information on dimensions and geometries of the channel have been generated and can be used for quality control before assembly of the individual parts, increasing the efficiency of manufacturing.

There are limitations in general applicability of the proposed procedure to parts having high-sloped surfaces and undercuts (i.e. re-entrant surfaces) because those geometrical features cannot be acquired by optical microscopy. This limits the range of geometries that can be successfully characterised. However, since channel-like geometries are extensively used in different applications, the methodology presented in this work can be extended to the characterization and quality inspection of other micro fabricated parts and devices.

Acknowledgements

Dr. Federica Michelin and Prof. Nicola Elvassore, both University of Padova - DII, Italy, are thanked for providing the microfluidic case study and insightful discussions on the functionality of micro-valves and their failure modes.

References

Whitesides GM. (2006) The origins and the future of microfluidics. Nature 442: 368-373.

Oh CK., Lee SW., Jeong OC. (2015) Fabrication of pneumatic valves with spherical dome-shape fluid chambers. Microfluidics and Nanofluidics 19: 1091-1099.

McDonald JC., Whitesides GM. (2002) Poly(dimethylsiloxane) as a material for fabricating microfluidic devices. Accounts of chemical research 35 (7): 491-499.

Unger MA., Chou H., Thorsen T., Scherer A., Quake SR. (2000) Monolithic Microfabricated Valves and Pumps by Multilayer Soft Lithography. Science 288: 113-116.

Eddings MA., Gale BK. (2006) A PDMS-based gas permeation pump for on-chip fluid handling in microfluidic devices. J Micromech Microengineering 16: 2396-2402.

Studer V., Hang G., Pandolfi A., Ortiz M., Anderson WF., Quake SR. (2004) Scaling properties of a low-actuation pressure microfluidic valve. J. Appl. Phys 95: 393-8.

Prevedello L, Michielin F, Balcon M, Savio E, Pavan P, Elvassore N (2018) A Novel Microfluidic Platform for Biomechano-Stimulations on a Chip. Ann Biomed Eng. doi: 10.1007/s10439-018-02121-z

Carmignato S, Voltan A, Savio E. (2010). Metrological performance of optical coordinate measuring machines under industrial conditions. CIRP ANNALS, vol. 59/1:497-500, ISSN: 0007-8506, doi: 10.1016/j.cirp.2010.03.128

Savio E., Marinello F., Bariani P., Carmignato S. (2007) Feature-Oriented Measurement Strategy in Atomic Force Microscopy. CIRP Annals 56/1: 557-560.

Marinello F, Savio E., Carmignato S, De Chiffre L. (2008). Calibration artefact for the microscale with high aspect ratio: The fiber gauge. CIRP ANNALS. vol. 57/1, pp. 497-500 ISSN: 0007-8506. doi:10.1016/j.cirp.2008.03.086.

Dixson R, Orji N., Misumi I., Dai G. (2018) Spatial dimensions in atomic force microscopy: Instruments, effects, and measurements. Ultramicroscopy, Volume 194, November 2018, Pages 199-214

Leach RK (2011) Optical Measurement of Surface Topography. Springer-Verlag, Berlin Heidelberg.

Senin, N. and L. Blunt (2013) *Characterisation of Individual Areal Features.* In: *Characterisation of Areal Surface Texture*, R.K. Leach Editor, Springer, Heidelberg, pp 179-216.

Senin, N., L.A. Blunt, and M. Tolley (2012) Dimensional metrology of micro parts by optical three-dimensional profilometry and areal surface topography analysis. Proc. IMechE Part B: J. of Engineering Manufacture 226 (11): pp 1819-1832

ISO 17450-1:2011 Geometrical product specifications (GPS) - General concepts - Part 1: Model for geometrical specification and verification.

Gonzalez RC., Woods RE. (2007) Digital Image Processing 3rd edition, Prentice Hall, New Jersey

Medeossi F, Sorgato M, Bruschi S, Savio E (2018) Novel method for burrs quantitative evaluation in micro-milling. Precision Engineering DOI: 10.1016/j.precisioneng.2018.07.007

Balcon M., Carmignato S., Savio E. (2012) Performance verification of a confocal microscope for 3D metrology tasks. Quality - Access to Success 13: pp 63-66.

Barker R. (2004) Guide to EUROMETROS: a manual for users, contributors, and testers. National Phisical Laboratory

ISO 25178-6: 2010 Geometrical product specifications (GPS) - Surface texture: Areal - Part 6: Classification of methods for measuring surface texture.

ISO 25178-602: 2010 Geometrical product specifications (GPS) - Surface texture: Areal - Part 602: Nominal characteristics of non-contact (confocal chromatic probe) instruments.

Jiang J., Scott PJ., Whitehouse DJ., Blunt L. (2007) Paradigm shifts in surface metrology. Part II. The current shift. Proceedings of the Royal Society of London, Series A (Mathematical, Physical and Engineering Sciences) 463: pp 2071-99.

Blunt L., Xiao S. (2011) The use of surface segmentation methods to characterise laser zone surface structure on hard disc drives. Wear 271: pp 604-609.

Senin N., Blunt L., Tolley M. (2012) The use of areal surface topography analysis for the inspection of micro-fabricated thin foil laser targets for ion acceleration. Measurement Science and Technology 23.

De Chiffre L., Carmignato S., Kruth J.P., Schmitt R., Weckenmann A. (2014) Industrial applications of computed tomography. CIRP Annals 63/2: pp 655-677.

Ontiveros S., Yague-Fabra J.A., Jimenez R., Tosello G., Gasparin S., Pierobon A., Carmignato S., Hansen H.N. (2012) Dimensional measurement of micro-moulded parts by computed tomography. Measurement Science & Technology 23: 125401.

Wang J., Jiang X., Blunt L., Leach RK., Scott PJ. (2012) Intelligent sampling for the measurement of structured surfaces. Measurement Science and Technology 23.

Wang J., Jiang X., Blunt L., Leach RK., Scott PJ. (2011) Efficiency of adaptive sampling in surface texture measurement for structured surfaces. Journal of Physics: Conference Series 311.

Hansen HN., Tosello G., Gasparin S., De Chiffre L. (2011) Dimensional metrology for process and part quality control in micro manufacturing. International Journal of Precision Technology 2: pp 118-35.

Savio E. (2012) A methodology for the quantification of value-adding by manufacturing metrology. CIRP Annals 61/1: pp 503-506.

Savio E., De Chiffre L., Carmignato S., Meinertz J., (2016) Economic benefits of metrology in manufacturing, CIRP Annals, in press.

Hocken J., Pereira H.P., (2017), Coordinate measuring machines and systems, CRC Press